ACCOUNTS
of chemical research

The Effects of Confinement inside Carbon Nanotubes on Catalysis

XIULIAN PAN* AND XINHE BAO*

State Key Laboratory of Catalysis, Dalian Institute of Chemical Physics, Chinese Academy of Sciences, Zhongshan Road 457, Dalian 116023, China

RECEIVED ON DECEMBER 13, 2010

CONSPECTUS

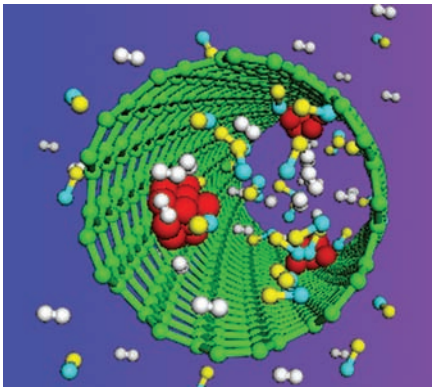

The unique tubular morphology of carbon nanotubes (CNTs) has triggered wide research interest. These structures can be used as nanoreactors and to create novel composites through the encapsulation of guest materials in their well-defined channels. The rigid nanotubes restrict the size of the encapsulated materials down to the nanometer and even the subnanometer scale. In addition, interactions may develop between the encapsulated molecules and nanomaterials and the CNT surfaces. The curvature of CNT walls causes the π electron density of the graphene layers to shift from the concave inner to the convex outer surface, which results in an electric potential difference. As a result, the molecules and nanomaterials on the exterior walls of CNTs likely display different properties and chemical reactivities from those confined within CNTs. Catalysis that utilizes the interior surface of CNTs was only explored recently. An increasing number of studies have demonstrated that confining metal or metal oxide nanoparticles inside CNTs often leads to a different catalytic activity with respect to the same metals deposited on the CNT exterior surface. Furthermore, this inside and outside activity difference varies based on the metals used and the reactions catalyzed.

In this Account, we describe the efforts toward understanding the fundamental effects of confining metal nanoparticles inside the CNT channels. This research may provide a novel approach to modulate their catalytic performance and promote rational design of catalysts. To achieve this, we have developed strategies for homogeneous dispersion of nanoparticles inside nanotubes. Because researchers have previously demonstrated the insertion of nanoparticles within larger nanotubes, we focused specifically on multiwalled carbon nanotubes (MWCNTs) with an inner diameter (i.d.) smaller than 10 nm and double-walled carbon nanotubes (DWCNTs) with 1.0−1.5 nm i.d. The results show that CNTs with well-defined morphology and unique electronic structure of CNTs provide an intriguing confinement environment for catalysis.

Introduction

CNTs can be envisioned as rolled-up graphene layers forming a tubular structure. According to the number of layers, single-walled CNTs (SWCNTs), double-walled CNTs (DWCNTs), and multiwalled CNTs (MWCNTs) are distinguished. Their high electron and thermal conductivity, high surface area, and functionalizable surfaces have evoked wide interest for catalytic applications.[1,2] For example, MWCNTs were reported to catalyze oxidative dehydrogenation of ethylbenzene to styrene due to the presence of surface oxygen functional groups.[3] As a catalyst additive, MWCNTs promoted substantially the catalytic activities of CuZnAl and CoMoCu for methanol and mixed alcohol synthesis, respectively.[4] Inspired by the successful applications of activated carbon (AC) as a catalyst support in industrial processes, CNTs were widely studied as an alternative for dispersion of transition metals on their exterior walls for hydrogen involving reactions and electrocatalytic reactions. A general conclusion can be drawn from those studies that the activity or product selectivities are improved in comparison to the metals supported on AC and conventional oxides.[1,2]

However, catalysis utilizing the interior surface of CNTs has been less explored,[5,6] although theoretical studies predicted that chemical reactions (without additional catalysts) may be influenced inside such a significantly

Published on the Web 06/27/2011 www.pubs.acs.org/accounts
10.1021/ar100160t

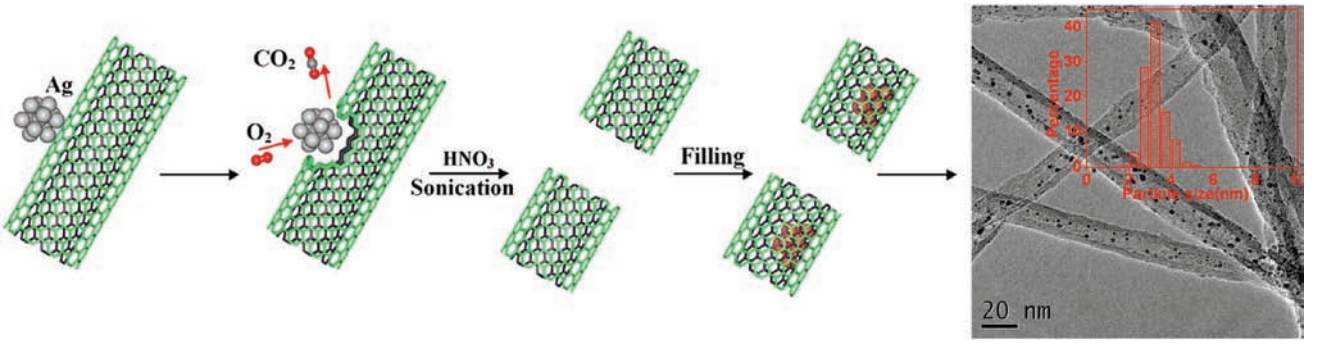

FIGURE 1. Scheme for introducing nanoparticles inside MWCNTs (i.d. 4−8 nm) by a wet chemistry method. The TEM image displays Ru nanoparticles confined in MWCNTs with the inset showing their particle size distribution.

reduced reaction volume, for example, the D exchange with H_2.[7] The Menshutkin reaction yielding the charged product ($[H_3NCH_3]^+[Cl]^-$)[8] also benefited from enclosure inside CNTs due to dipolar interaction of the product and CNT surface. In addition, confinement has been demonstrated to modify the structure and properties of confined materials. For instance, water molecules formed a layered cylindrical structure consisting of hydrogen-bonded heptagonal rings inside nanotubes, which does not exist in the bulk phase.[9] Fe−Ni alloys crystallized inside CNTs exhibited several unusual morphological, compositional, and structural features.[10] Therefore, the CNT channels are anticipated to provide an intriguing confinement environment for metal catalysts and catalytic reactions.

Studying confinement effects in catalysis requires effective techniques to disperse metal nanoparticles uniformly inside the CNT channels. This has remained a challenge at a practical macroscale, in particular inside small nanotubes. Therefore, the first section of this Account is dedicated to recent developments in introducing nanoparticles within small nanotubes before experimental studies on catalytic reactions over CNT-confined metal nanoparticles are discussed, and finally the different effects on catalysis are considered.

Dispersion of Nanoparticles inside CNTs

The efforts to fill the CNT channels started shortly after their discovery and several techniques were developed including in situ filling during arc discharge, vapor deposition of volatile complexes, and wet chemistry methods.[11−16] Wet chemistry methods are simple and most versatile for catalysis since they are applicable to most metals. The filling depends on the surface tension of the liquid and the contact angle between the liquid and the pore walls. CNTs were predicted to be wettable by liquids with a surface tension below 100−200 mN/m and thus could be filled through open ends.[13] Discrete nanoparticles of various metals had been successfully introduced inside the CNT channels with a few tens of nanometer width.[14,15] However, difficulties were often encountered in small tubes with an inner diameter (i.d.) of a few nanometers. For example, Ugarte et al. observed that nanotubes with a diameter smaller than 3 nm were barely filled due to the size constraint on the capillarity and the wetting behavior.[16] Yet, small nanotubes are anticipated to be more interesting for catalysis because one may obtain metal particles in this size range and even down to a sub-nanometer scale due to the space restriction. Extraordinary catalytic activities have been frequently demonstrated for metal particles at this scale, for example, Au[17] and Ag.[18]

We have improved the wet chemistry method and achieved homogeneous dispersion inside small MWCNTs (i.d. 4−8 nm).[19] As depicted in Figure 1, the freshly produced MWCNTs were opened at the ends and shortened via a controlled oxidation process catalyzed by Ag nanoparticles. Shortened tubes reduce the transport resistance for the metal precursor solutions into the channels, as well as for reactants and products if reactions take place inside the channels. Ultrasonic treatment and stirring were employed to facilitate the expulsion of the air and the entry of solution in the channels. Take filling of CNTs with Ru particles as an example, a $RuCl_3$/acetone solution was employed. TEM indicated that around 80% of Ru particles were distributed inside the channels following drying and reduction in H_2,[20] which was confirmed by three-dimensional tomography.[21] The particles had a rather narrow size distribution with 90% falling in the range of 2−4 nm. Following the same method, iron[22,23] and rhodium[24] have been dispersed within MWCNTs too, demonstrating that this can be applied for many transition metals. The MWCNT-confined metal particles

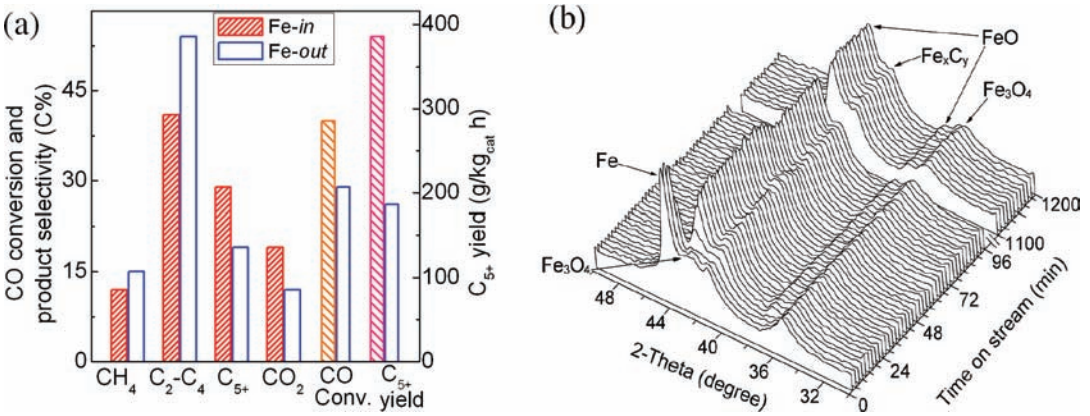

FIGURE 2. (a) The effect of confinement in CNTs on the activity of FTS iron catalyst and (b) crystal-phase evolution of Fe-*in* in syngas.[23]

are labeled as Metal-*in*, and metal particles located on the outside of CNTs as Metal-*out* in the following.

We found that filling of DWCNTs (i.d. 1−2 nm) was not very successful with the just described wet chemistry method. Instead, using $TiCl_4$ vapor, we successfully dispersed subnanometer-sized titania particles in DWCNTs.[25] Nanotubes were first evacuated before exposure to $TiCl_4$. Anhydrous ethanol was used to affect slow hydrolysis of $TiCl_4$ under Ar atmosphere. A small amount of titanium species on the outer walls was removed by hydrofluoric acid followed by washing with deionized water. The bright dots in the high-angle annular−dark field (HAADF) electron microscopy (providing sub-angstrom resolution) image corresponding to heavy element titanium were neatly aligned in the resulting sample, and the size of the majority was around 0.2 nm, even though some were probably bigger under the microscope due to overlapping of individual dots. Larger particles were only observed inside a few bigger nanotubes. These particles exhibited a rather good stability since no obvious aggregation was observed under the electron microscope when the sample was in situ heated up to about 500 °C.[25] This method is expected to enable synthesis of other sub-nanometer-sized metal and metal oxide clusters. To distinguish from MWCNT samples, titania confined inside DWCNTs are labeled as TiO_x-*in*-D, and the outside catalysts are denoted as TiO_x-*out*-D.

Gas-Phase Reactions

Syngas Conversion. The confinement effect on Fischer−Tropsch synthesis (FTS) was studied by comparing iron confined (Fe-*in*) in MWCNTs (i.d. 4−8 nm) and on their outside (Fe-*out*).[23] TEM analysis indicated that over 70% of iron particles of Fe-*in* were distributed inside CNT channels while almost all particles of Fe-*out* were on the outside. This

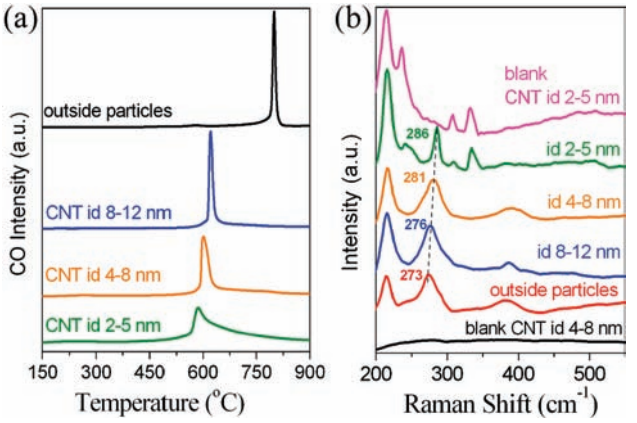

FIGURE 3. (a) Temperature-programmed desorption profiles in He for the CNT-confined Fe_2O_3 particles with different inner diameters where Fe_2O_3 is reduced by carbon from CNTs and (b) their Raman spectra.[22]

CNT-confined catalyst favored CO conversion and formation of long chain hydrocarbons. For example, CO conversion was almost 1.5 times, and the yield of C_{5+} hydrocarbons was twice as high as those over Fe-*out* at 6000 h^{-1}, and 5 MPa (Figure 2a).[23] Furthermore, the yield was 6 times higher than that over the XC-72 carbon black supported iron catalyst, which had a similar surface area as the MWCNTs.

In situ HRTEM, XRD, Raman spectroscopy, and temperature-programmed desorption (TPD) experiments revealed that the reduction of Fe_2O_3 particles by CNTs was facilitated within MWCNTs with respect to the outside oxide.[22,26] The narrower the tubes, the more facile was the reduction of the confined Fe_2O_3 (Figure 3a). Facilitated reduction was also observed for Fe_3O_4 nanowires inside CNTs.[27] Even in H_2 and CO,[23] the reduction of the confined Fe_2O_3 nanoparticles to FeO and metallic Fe occurred at a ca. 60−90 °C lower temperature than that for the outside catalyst at each step. This facilitated reduction of metal oxide induced by

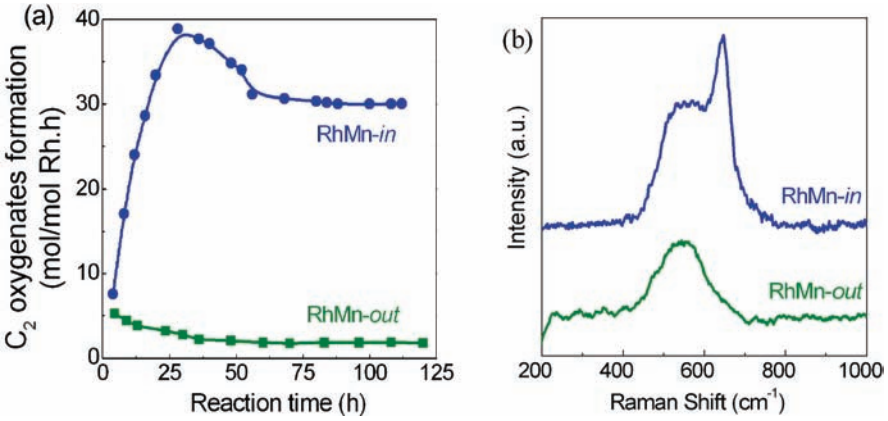

FIGURE 4. (a) Syngas conversion to C_2 oxygenates over RhMn catalysts; (b) Raman spectra for RhMn catalysts upon in situ CO adsorption.

confinement in CNTs appears to be a general phenomenon because a similar trend was observed for ruthenium[20] and cobalt.[28]

Raman spectroscopy showed that the Fe−O band red-shifted for the outside Fe_2O_3 particles with respect to bulk Fe_2O_3.[22] However, it blue-shifted for the CNT-confined Fe_2O_3 particles compared with the outside oxide. The blue shift became stronger with decreasing inner diameter (Figure 3b). Although the particle size declined with the downsized CNT channels, the stepwise blue shift of the Fe−O band contrasts with the red shift generally reported for nanosized Fe_2O_3. Confinement of manganese oxide also resulted in a blue shift of the Mn−O frequency by 6 cm^{-1} compared with the outside MnO_2 particles.[29] These observations imply there might be interactions between the confined metal oxides and the CNT surface.

In situ XRD (Figure 2b) showed that the improved reducibility of Fe-*in* favored the formation of more iron carbides under reaction conditions, which are generally accepted as the catalytically active phase for FTS synthesis.[30] Therefore, the higher activity of Fe-*in* could be attributed to the confinement inside CNTs, which prevented iron particles from severe sintering and facilitated the reduction of iron oxide to form iron carbides.

A better reducibility and an enhanced catalytic performance of CNT-confined iron (Fe-*in*) were also observed by Dalai and co-workers.[31] Their Fe-*in* catalyst had 70−80% Fe particles located inside CNTs with a particle size of 6−11 nm, while their Fe-*out* had slightly smaller particles (5−9 nm). Both catalysts exhibited a similar initial CO conversion at 2 MPa and space velocity of 2 L/(g h). However, Fe-*in* was much more stable as CO conversion was 6%−10% higher than that over Fe-*out* in the temperature range of 265−285 °C, and selectivity to C_{5+} hydrocarbon products was higher by 13% after 125 h time on stream.[31] The above results indicate that the FTS activity difference between inside and outside catalysts is sensitive to pressure and space velocity.

Confinement of a bicomponent RhMn catalyst in CNT channels (RhMn-*in*) was also found to enhance its catalytic activity for syngas conversion to C_2 oxygenates with respect to the outside catalyst (RhMn-*out*) (Figure 4a).[24] TEM indicated that the particle size was not the only factor affecting the activity because the two fresh catalysts had similar size distributions. The catalyst supported on SBA-15, which has a pore diameter (6−8 nm) similar to that of the used CNTs, exhibited a much lower activity and a higher selectivity to the byproduct methane under the same reaction conditions. This suggested that the spatial restriction may not be the sole effect. In addition to likely increased local density of reactants within small channels, Raman spectra (Figure 4b) indicated that the activation of CO may have been modified inside CNTs.[24] Two Raman bands corresponding to the Rh−C (~550 cm^{-1}) and Mn−O (~640 cm^{-1}) bonds were observed for RhMn-*in* but only one for RhMn-*out* when both catalysts were exposed to CO. This was likely the result of the different interaction of the metals with CNTs. The oxophilic Mn may remain in a more reduced state inside the CNT channels with respect to the outside Mn species. Thus Mn could attract the O of CO adsorbed on adjacent Rh sites, leading to a tilted adsorption with the C atom bonding to Rh and O to Mn inside CNTs, which could facilitate CO dissociation. In contrast, the tendency of outside Mn to attract the O of CO could be weaker and hence a lower CO dissociation activity.

Ammonia Synthesis and Ammonia Decomposition. Confinement inside CNTs can also have a negative impact on the catalytic activity, as we have observed for ammonia synthesis over Ru catalysts.[20] The turnover frequency (TOF)

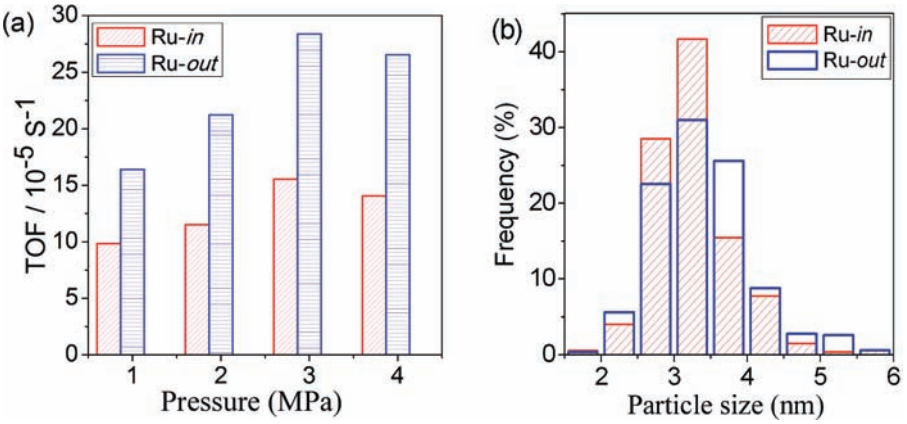

FIGURE 5. (a) Ammonia synthesis activity and (b) particle size distributions of Ru-*in* and Ru-*out*.

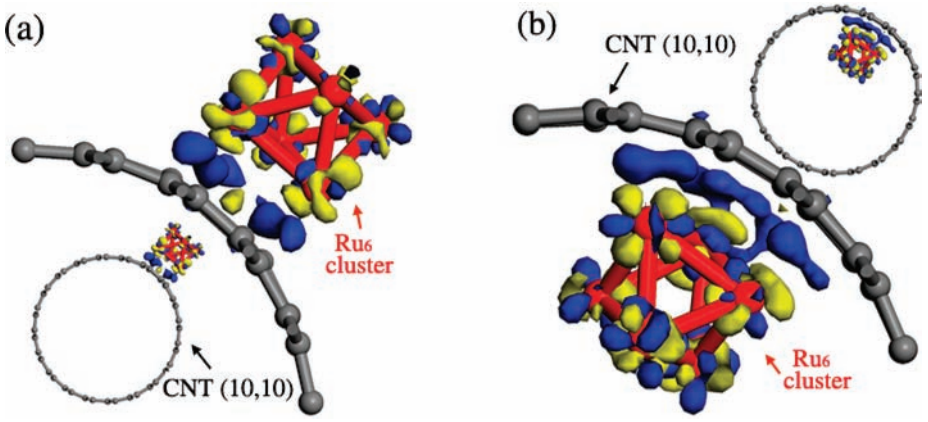

FIGURE 6. The differential electron density isosurfaces of (a) Ru_6-*out* and (b) Ru_6-*in*. The insets show the cross-section of a full nanotube model. The gray balls represent the carbon atoms and red bars the Ru−Ru bonds. The blue and yellow areas suggest enriched and depleted electron density, respectively, with respect to free-standing clusters.

over Ru-*in* was in the range of $(1.6-2.6) \times 10^{-4}$ s^{-1} at 400 °C and 20 mL·min^{-1} flow rate in the pressure range of 1−4 MPa. Remarkably, TOFs over Ru-*out* were much higher (Figure 5a).[20] TEM and chemisorption experiments confirmed that the particle size of Ru-*in* and Ru-*out* was similar, with ∼90% particles falling in the range of 2−5 nm (Figure 5b). Even after reaction, the particle size distribution only changed slightly, indicating that both catalysts were rather stable under reaction conditions.

Adsorption microcalorimetry showed that the initial differential heat for CO adsorption on Ru-*out* was 12 kJ/mol higher than that over Ru-*in*.[20] This implied stronger adsorption sites for CO on Ru-*out*. The different strength of adsorption sites was most likely related to the electron density on metal surfaces since Ru-*in* and Ru-*out* had a similar particle size. This was corroborated by first principles calculations.[20] Figure 6 shows the differential electron density isosurfaces of a Ru_6 cluster inside (Ru_6-*in*) and outside (Ru_6-*out*) of a SWCNT(10,10).[20] Mulliken population analysis indicated that the Ru_6-*out* cluster donated 1.66 electrons to the CNT convex surface whereas the inside cluster transferred 2.41 electrons to the concave surface. This is consistent with the electron structure of CNTs. Deviation from planarity causes π-electron density to shift from the concave interior to the convex exterior surface.[32,33] Thus, the outside metal cluster donates less electrons to the relatively electron-enriched exterior surface than the inside cluster to the electron-deficient interior surface. These results could explain the higher ammonia synthesis activity over Ru-*out* than over Ru-*in* since a higher electron density facilitates the electrophilic process of N_2 dissociative adsorption.[34]

On the other hand, it was recently reported that ammonia decomposition benefits from confinement of the bimetal $CoFe_5$ inside CNTs with 40 nm average i.d. ($CoFe_5$-*in*).[35] TEM indicated that 96 wt % particles of $CoFe_5$-*in* were located inside the channels and $CoFe_5$-*out* had 73 wt % located on the outside. The two fresh catalysts exhibited a similar particle size distribution and the same $CoFe_2O_4$(311) planes.

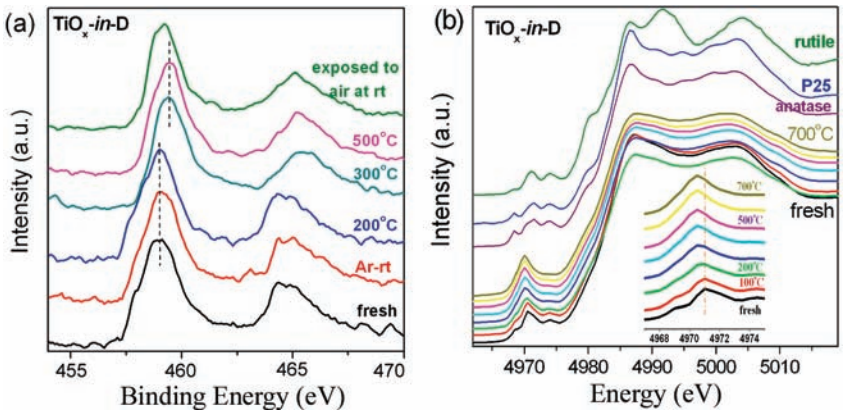

FIGURE 7. (a) Ti 2p XPS spectra and (b) XANES features of TiO_x-*in*-D as function of temperature.

NH_3 conversion over $CoFe_5$-*out* was roughly half of that over $CoFe_5$-*in* during ~16 h time on stream. The superior thermal stability of the inside particles was proposed to be responsible for their higher conversion.[35] The electron transfer within the graphene walls is expected to be much smaller in large CNTs because of their weaker curvature.[32,33] Thus it likely has little influence on the electronic structure of metal particles inside wide CNTs. The above results show that the activity difference between the inside and outside catalysts differs in ammonia synthesis and decomposition. This could be due to confinement effects on different metals in different diameter CNTs.

Epoxidation of Propylene in DWCNTs. Subnanometer titania clusters confined inside DWCNT channels (TiO_x-*in*-D) exhibited a significantly higher activity for catalyzing propylene epoxidation compared with titania outside of DWCNTs (TiO_x-*out*-D) and titania inside MWCNTs (i.d. 4−8 nm) (TiO_x-*in*)[25] The formation rate of propylene oxide (PO) over TiO_x-*in*-D was 54.0 g PO/(kg cat·h). It was 8 times higher than that over TiO_x-*out*-D, twice as high as that over TiO_x-*in*, and more than 20 times higher than titania supported on commercial P25 under the same reaction conditions. Note that no conversion was detected over blank DWCNTs.

X-ray photoelectron spectroscopy (XPS), X-ray absorption near-edge spectroscopy (XANES), and Raman spectroscopy suggested an electronic interaction between the confined titania clusters and the DWCNT interior wall.[25] This electron transfer was temperature dependent and was strong enough to be observed above 300 °C. For example, the Ti 2p XPS peak shifted 0.5 eV to a higher binding energy for TiO_x-*in*-D (Figure 7a), whereas that of TiO_x-*out*-D did not exhibit any changes. Correspondingly, the 4970.5 eV peak in the pre-edge region also downshifted to 4970.0 eV for TiO_x-*in*-D at 300 °C (Figure 7b) suggesting a lower Ti 3d electron density since the XANES result from the 1s → 3d dipole transition. The modified electronic structure and the stabilization of small clusters might contribute to the higher epoxidation activity for TiO_x-*in*-D.

Liquid-Phase Hydrogenation Reactions

Dependence of catalytic activity on the relative location of catalysts on CNTs was first noticed in liquid-phase hydroformylation of propylene.[36] A catalyst consisting of a $[HRh(CO)(PPh_3)_3]$ complex deposited on open CNTs yielded a TOF = 0.10 s^{-1} and a molar ratio of the normal/branched products n/i = 9 in comparison to 0.06 s^{-1} (TOF) and n/i = 6 over the complex on closed CNTs. Although no direct evidence was provided for the location of Rh, the higher activity and regioselectivity of the open catalyst were suggested to be attributed to the Rh species inside CNTs and its surface consisting of six-membered C-rings.[36]

Pd particles were introduced inside MWCNTs (i.d. 5−10 nm) for benzene hydrogenation, which exhibited a TOF twice as high as that over zeolite Y and AC-supported Pd catalysts although zeolite Y and AC have much higher surface areas than CNTs.[37] Confinement of Pd particles inside MWCNTs (40 nm average i.d.) was also found to benefit selective hydrogenation of cinnamaldehyde with a faster hydrogenation rate and a much higher selectivity (90%) to hydrocinnamaldehyde compared with an AC-supported Pd catalyst.[38] Likewise Serp and co-workers observed a much better catalytic performance for PtRu particles inside MWCNTs (40 nm average i.d.) for the same reaction but with opposite selectivity.[15] The TOF was almost 3 times and the selectivity toward cinnamyl alcohol was more than twice of that over an unsupported PtRu catalyst with a similar particle size. Moreover, the selectivity was linearly correlated with the percentage of nanoparticles located inside CNTs.[15] A higher selectivity toward cinnamyl alcohol was also observed over

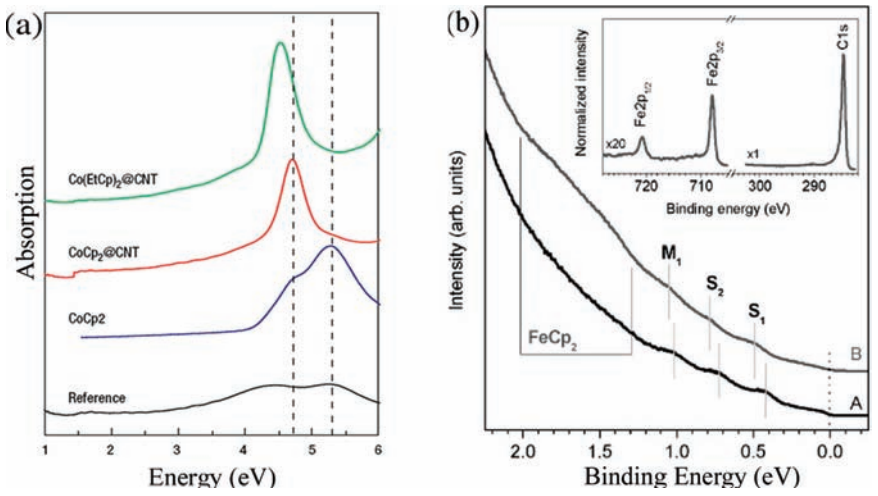

FIGURE 8. (a) UV−vis absorption spectra of SWCNT-confined [$CoCp_2$] indicating electron transfer from cobalt ions to the nanotube;[40] (b) ultraviolet photoemission spectroscopy of the SWCNT-confined [$FeCp_2$] (spectrum B) in comparison with that of pristine SWCNT (spectrum A).[41]

a CNT-confined Pt catalyst (60−100 nm i.d.) compared with the outside Pt catalyst.[39]

Toward Understanding the Confinement Effects in Catalysis

Electronic Interaction of the Confined Materials with CNTs. The effect of the electronic structure of CNTs on the transition states of a chemical reaction has been theoretically studied ealier.[8] In addition, modified redox behavior of metals and metal oxides, as demonstrated in the previous section, implied interactions between the confined materials and CNT surfaces.[20,23,26,27,31] Our CO adsorption microcalorimetry and first principles calculation results suggested that the inside Ru transferred more electrons to the CNT interior surface than the outside Ru to the exterior surface.[20] Such an electron transfer was observed experimentally for CNT-confined metallocene molecules. For example, Khlobystov and co-workers attributed a red-shift of the photoluminescence and UV−vis absorption spectra of CNT-encapsulated bis(cyclopentadienyl) cobalt [$CoCp_2$] and bis(ethylcyclopentadienyl) cobalt molecules [$Co(EtCp)_2$] (Figure 8a) to a change of the cobalt charge state due to electron transfer to the nanotubes.[40] Similarly, Shiozawa et al. estimated that 0.14 electrons were transferred from confined [$FeCp_2$] to SWCNTs per [$FeCp_2$] molecule according to a shift to a higher binding energy in the ultraviolet photoemission spectra (Figure 8b).[41] Lee et al. observed a modified electronic structure of the nanotube in CNT-encapsulated Gd metallofullerenes, as evidenced by low-temperature scanning tunneling microscopy.[42]

The above results demonstrate that an electronic interaction exists between metal species and the CNT surfaces and the strength can vary with metals and with the size of CNTs. The modified electronic structure of metal/metal oxide nanoparticles induced by confinement can influence their catalytic activity as redox reactions involve electron transfer between reactants and catalysts.

Space Restriction. The nanosized channels of CNTs provide spatial restriction on metal particles, which can hamper their aggregation under reaction conditions. This is important because aggregation of nanoparticles frequently results in deactivation of catalysts. For example, the particles of RhMn-*in* were limited to the range of 5−8 nm in CNTs even after 112 h time on stream, which led to a rather steady performance at syngas conversion conditions of 320 °C and 5 MPa.[24] In contrast, the particles of RhMn-*out* aggregated noticeably as indicated by a broader distribution of 8−10 nm size due to lack of space restriction. The superior stability of the confined nanoparticles was also observed for FTS iron catalyst.[31] The inside particles remained in the range of 6−11 nm while the outside particles grew and the largest particles reached 24 nm after 125 h time on stream.

Furthermore, the availability of nanotubes with varying inner diameters enables tuning the particle size. For example, inside small tubes such as DWCNTs, subnanometer titania particles had been well dispersed.[25] The capability of creating variable nanometer-sized metal particles and maintaining their high dispersity under reaction conditions makes CNTs interesting support materials and could trigger further fundamental investigations on the nature of nanocatalysis.

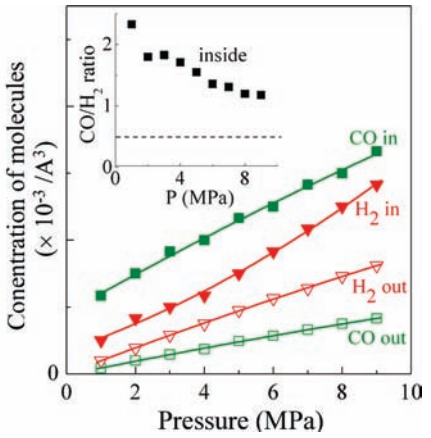

FIGURE 9. The concentration of CO and H_2 molecules inside and outside of SWCNT(10, 10) channels as a function of pressure. The inset shows the CO/H_2 ratio inside SWCNTs with the dashed line indicating the bulk ratio.[43]

Enrichment of Reactants inside CNTs. Molecules such as H_2, alkanes, alkenes, and carbon tetrachloride have been reported to bind more strongly on the interior surface of CNTs.[9] Combining first principles calculations with Monte Carlo (MC) simulation, we showed that both CO and H_2 molecules are enriched in a pressure range 1−9 MPa inside SWCNT channels as a consequence (Figure 9).[43] Furthermore, CO was more enriched than H_2 due to stronger interaction of CO with the CNT interior surface resulting in a CO/H_2 ratio higher than that in the bulk syngas feed. This enrichment generally became greater inside smaller nanotubes. The increased concentration of CO and H_2 could help accelerate the reaction rate, and the altered ratio of CO/H_2 could also lead to modified product selectivities.

Diffusion inside CNT channels. When the mean free path of molecules is larger than the tube diameters and the density of the gas is low, the transport follows the Knudsen diffusion mechanism, which is characterized by a diffusion rate 2−3 orders of magnitude lower than that in the gas phase. This may cause severe transport resistance in catalytic reactions. The diffusion inside CNTs has been studied employing solid-state nuclear magnetic resonance (NMR) using hyperpolarized ^{129}Xe as the probe molecule.[44]

When SWCNTs (i.d. 2−2.5 nm) preadsorbed with ^{129}Xe were exposed to a mixture of ^{129}Xe and methanol (the switch-on sign in Figure 10), methanol gradually drove ^{129}Xe out of and occupied the channels. Consequently the intensity of the ~66 ppm resonance corresponding to the inside ^{129}Xe declined. When methanol was switched off, the intensity of ^{129}Xe increased due to desorption of methanol (Figure 10). From this intensity change during methanol

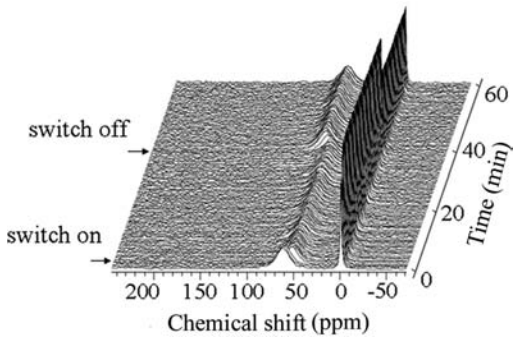

FIGURE 10. NMR spectra for the ^{129}Xe signal at ~66 ppm inside SWCNTs during adsorption and desorption of methanol at 0 °C. The 0 ppm signal results from gas-phase ^{129}Xe.

adsorption and desorption, the methanol diffusion rate was estimated to be ten times as high as that inside MCM-41, which has a comparable pore size (~3 nm). The fast diffusion rate within CNTs was probably due to low friction and weakened hydrogen bonds among methanol molecules. MC and molecular dynamic simulation confirmed faster diffusion coefficient of methanol in a SWCNT (10, 10) than in the pores of VFI zeolite (1.5 nm in size).[44] More rapid diffusion of other molecules in CNTs than other nanoporous materials has also been reported earlier.[45]

Conclusions and Prospects

The well-defined nanosized channels of CNTs formed by graphene layers provide an intriguing confinement environment for catalysis. They not only exert a spatial restriction on metal particles hampering their sintering but also make it possible to tune the particle size simply by changing the channel diameters. For example, subnanometer-sized clusters can be obtained within SWCNTs and DWCNTs. The electronic interaction of the confined catalysts with the CNT walls modifies their properties, which can influence the adsorption activation of reactants and hence the catalytic activity. In addition, the interaction between the reactants and the CNT surface can modify the diffusion behavior and lead to enriched reactants inside the CNT channels, which create further opportunities to modulate the catalytic performance. These effects may influence reaction rates to different extents depending on the selected metals, the diameter of CNTs and specific reactions. Insights into the nature of such confinement effects could provide a novel approach to tune the catalytic activity or selectivity.

In addition to the CNT diameters, the confinement effect can be further modulated by modifying the electronic structure of the curved graphene walls. This can be achieved by doping CNTs with heteroatoms. For instance, doping with

boron introduced acceptor states near the valence band edge[46] while nitrogen-doping added electron donor states near the conduction band edge.[47] N-doped MWCNTs were recently demonstrated to enhance significantly the ammonia decomposition activity of Ru nanoparticles dispersed on their exterior walls.[48] Precise manipulation of the location of heteroatoms either exclusively on interior or exterior walls of CNTs may allow fine-tuning of catalytic properties.

Looking beyond CNTs, spherical fullerenes such as buckminsterfullerene C_{60} may provide another intriguing confinement environment because of their well-defined cavities, which allow trapping of only a few metal atoms. Their large curvature may induce a strong interaction between the metal clusters and carbon surface. For example, electron transfer from encapsulated metal atoms such as Sc, Tm, and La to the cage was reported leading to a narrowed bandgap compared with the empty fullerenes.[49] However, encapsulation of transition metal atoms and the effects on catalysis are yet to be explored.

The potential of CNTs as alternative catalytic supports has been demonstrated, and the commercial availability in large scale has also brought CNTs one step closer to applications. However, challenges remain with fabrication of technical CNT-based catalysts mainly due to the shaping difficulties. Successful growth of CNTs on silica spheres,[50] alumina particles,[51] and inert SiC substrates[52] recently may offer a possible solution since silica, alumina, and SiC are compactable and have been used as catalyst supports in industrial processes.

BIOGRAPHICAL INFORMATION

Xiulian Pan received her Ph.D. from the Dalian Institute of Chemical Physics (DICP) in 2001 after carrying out a thesis on palladium hollow fiber membranes for hydrogen separation and membrane catalysis under the guidance of Prof. Guoxing Xiong. After 2 years as a postdoctoral fellow at the Fraunhofer Institute for Interfacial Engineering and Biotechnology in Stuttgart (Germany), she joined Prof. Xinhe Bao's group at the State Key Laboratory of Catalysis of DICP, where she was appointed full professor in 2009. Her current research interests involve nanostructured carbon for catalysis, including carbon nanotubes, graphene, and ordered mesoporous carbons.

Xinhe Bao received his Ph.D. in Physical Chemistry from Fudan University in China in 1987. He held an Alexander von Humboldt Research Fellow position in Frize-Haber institute between 1989 and 1995, hosted by Prof. Gerhard Ertl. Following that, he joined the Dalian Institute of Chemical Physics as a full Professor. He became a member of the Chinese Academy of Sciences in 2009. His research activities focus on the fundamental study of catalysis, including development of new catalysts and novel catalytic processes related to energy. Currently, his attention is focused on "nanocatalysis" with emphasis on the development of science and techniques to assemble and stabilize nanostructured particles using porous materials and carbon nanotubes.

We acknowledge the financial support of the National Science Foundation of China (Projects 11079005 and 21033009).

FOOTNOTES

*E-mail addresses: panxl@dicp.ac.cn; xhbao@dicp.ac.cn.

REFERENCES

1 De Jong, K. P.; Geus, J. W. Carbon nanofibers: Catalytic synthesis and applications. *Catal. Rev.* **2000**, *42*, 481–510.

2 Serp, P.; Corrias, M.; Kalck, P. Carbon nanotubes and nanofibers in catalysis. *Appl. Catal. A: Gen.* **2003**, *253*, 337–358.

3 Mestl, G.; Maksimova, N. I.; Keller, N.; Roddatis, V. V.; Schlogl, R. Carbon nanofilaments in heterogeneous catalysis: An industrial application for new carbon materials? *Angew. Chem., Int. Ed.* **2001**, *40*, 2066–2068.

4 Zhang, H.; Liang, X.; Dong, X.; Li, H.; Lin, G. Multi-walled carbon nanotubes as a novel promoter of catalysts for CO/CO_2 hydrogenation to alcohols. *Catal. Surv. Asia* **2009**, *13*, 41–58.

5 Pan, X.; Bao, X. Reactions over catalysts confined in carbon nanotubes. *Chem. Commun.* **2008**, 6271–6281.

6 Serp, P.; Castillejos, E. Catalysis in carbon nanotubes. *ChemCatChem* **2010**, *2*, 41–47.

7 Lu, T.; Goldfield, E. M.; Gray, S. K. Chemical reactivity within carbon nanotubes: A quantum mechanical study of the $D + H_2 \rightarrow HD + H$ reaction. *J. Phys. Chem. C* **2008**, *112*, 2654–2659.

8 Halls, M. D.; Schlegel, H. B. Chemistry inside carbon nanotubes: The Menshutkin S_N2 reaction. *J. Phys. Chem. B* **2002**, *106*, 1921–1925.

9 Kondratyuk, P.; Yates, J. T. Molecular views of physical adsorption inside and outside of single-wall carbon manotubes. *Acc. Chem. Res.* **2007**, *40*, 995–1004.

10 Golberg, D.; Gu, C. Z.; Bando, Y.; Mitome, M.; Tang, C. C. Peculiarities of Fe-Ni alloy crystallization and stability inside C nanotubes as derived through electron microscopy. *Acta Mater.* **2005**, *53*, 1583–1593.

11 Ajayan, P. M.; Ebbesen, T. W.; Ichihashi, T.; Iijima, S.; Tanigaki, K.; Hiura, H. Opening carbon nanotubes with oxygen and implications for filling. *Nature* **1993**, *362*, 522–525.

12 Guerret-Piecourt, C.; Lebouar, Y.; Loiseau, A.; Pascard, H. Relation between metal electronics-structure and morphology of metal - compunds inside carbon nanotubes. *Nature* **1994**, *372*, 761–765.

13 Ebbesen, T. W. Wetting, filling and decorating carbon nanotubes. *J. Phys. Chem. Solids* **1996**, *57*, 951–955.

14 Tessonnier, J. P.; Ersen, O.; Weinberg, G.; Pham-Huu, C.; Su, D. S.; Schlogl, R. Selective deposition of metal nanoparticles inside or outside multiwalled carbon nanotubes. *ACS Nano* **2009**, *3*, 2081–2089.

15 Castillejos, E.; Debouttiere, P. J.; Roiban, L.; Solhy, A.; Martinez, V.; Kihn, Y.; Ersen, O.; Philippot, K.; Chaudret, B.; Serp, P. An efficient strategy to drive nanoparticles into carbon nanotubes and the remarkable effect of confinement on their catalytic performance. *Angew. Chem., Int.Ed.* **2009**, *48*, 2529–2533.

16 Ugarte, D.; Chatelain, A.; deHeer, W. A. Nanocapillarity and chemistry in carbon nanotubes. *Science* **1996**, *274*, 1897–1899.

17 Valden, M.; Lai, X.; Goodman, D. W. Onset of catalytic activity of gold clusters on titania with the appearance of nonmetallic properties. *Science* **1998**, *281*, 1647–1650.

18 Lei, Y.; Mehmood, F.; Lee, S.; Greeley, J.; Lee, B.; Seifert, S.; Winans, R. E.; Elam, J. W.; Meyer, R. J.; Redfern, P. C.; Teschner, D.; Schlogl, R.; Pellin, M. J.; Curtiss, L. A.; Vajda, S. Increased silver activity for direct propylene epoxidation via subnanometer size effects. *Science* **2010**, *328*, 224–228.

19 Wang, C.; Guo, S.; Pan, X.; Chen, W.; Bao, X. Tailored cutting of carbon nanotubes and controlled dispersion of metal nanoparticles inside their channels. *J. Mater. Chem.* **2008**, *18*, 5782–5786.

20 Guo, S.; Pan, X.; Gao, H.; Yang, Z.; Zhao, J.; Bao, X. Probing the electronic effect of carbon nanotubes in catalysis: NH_3 synthesis with Ru nanoparticles. *Chem.—Eur. J.* **2010**, *16*, 5379–5384.

21 Friedrich, H.; Guo, S.; de Jongh, P. E.; Pan, X.; Bao, X.; deJong, K. P. A quantitative electron tomography study of Ru particles inside and outside of carbon nanotubes. *ChemSusChem* **201110.1002/cssc.201000325.**

22 Chen, W.; Pan, X.; Bao, X. Tuning of redox properties of iron and iron oxides via encapsulation within carbon nanotubes. *J. Am. Chem. Soc.* **2007**, *129*, 7421–7426.

23 Chen, W.; Fan, Z.; Pan, X.; Bao, X. Effect of confinement in carbon nanotubes on the activity of Fischer–Tropsch iron catalyst. *J. Am. Chem. Soc.* **2008**, *130*, 9414–9419.

24 Pan, X.; Fan, Z.; Chen, W.; Ding, Y.; Luo, H.; Bao, X. Enhanced ethanol production inside carbon-nanotube reactors containing catalytic particles. *Nat. Mater.* **2007**, *6*, 507–511.

25 Zhang, H.; Pan, X.; Liu, J.; Qian, W.; Wei, F.; Huang, Y.; Bao, X. Enhanced catalytic activity of subnanometer titania clusters confined inside double-wall carbon nanotubes. *ChemSusChem* **201110.1002/cssc.201000324.**

26 Chen, W.; Pan, X.; Willinger, M. G.; Su, D. S.; Bao, X. Facile autoreduction of iron oxide/carbon nanotube encapsulates. *J. Am. Chem. Soc.* **2006**, *128*, 3136–3137.

27 Cao, F.; Zhong, K.; Gao, A.; Chen, C.; Li, Q.; Chen, Q. Reducing reaction of Fe_3O_4 in nanoscopic reactors of a-CNTs. *J. Phys. Chem. B* **2007**, *111*, 1724–1728.

28 Trépanier, M.; Dalai, A. K.; Abatzoglou, N. Synthesis of CNT-supported cobalt nanoparticle catalysts using a microemulsion technique: Role of nanoparticle size on reducibility, activity and selectivity in Fischer–Tropsch reactions. *Appl. Catal. A: Gen.* **2010**, *374*, 79–86.

29 Chen, W.; Fan, Z.; Gu, L.; Bao, X.; Wang, C. Enhanced capacitance of manganese oxide via confinement inside carbon nanotubes. *Chem. Commun* **2010**, *46*, 3905–3907.

30 Raupp, G. B.; Delgass, W. N. Mössbauer investigation of supported Fe and FeNi catalysts: II. Carbides formed Fischer–Tropsch synthesis. *J. Catal.* **1979**, *58*, 348–360.

31 Abbaslou, R. M. M.; Tavassoli, A.; Soltan, J.; Dalai, A. K. Iron catalysts supported on carbon nanotubes for Fischer–Tropsch synthesis: Effect of catalytic site position. *Appl. Catal. A: Gen.* **2009**, *367*, 47–52.

32 Haddon, R. C. Chemistry of the fullerenes: The manifestation of strain in a class of continuous aromatic molecules. *Science* **1993**, *261*, 1545–1550.

33 Peralta-Inga, Z.; Lane, P.; Murray, J. S.; Boyd, S.; Grice, M. E.; O'Connor, C. J.; Politzer, P. Characterization of surface electrostatic potentials of some (5,5) and (n,1) carbon and boron/nitrogen model nanotubes. *Nano Lett.* **2003**, *3*, 21–28.

34 Aika, K.; Ozaki, A.; Hori, H. Activation of nitrogen by alkali-metal promoted transition metal. *J. Catal.* **1972**, *27*, 424–431.

35 Zhang, J.; Muller, J. O.; Zheng, W.; Wang, D.; Su, D. S.; Schlogl, R. Individual Fe-Co alloy nanoparticles on carbon nanotubes: Structural and catalytic properties. *Nano Lett.* **2008**, *8*, 2738–2743.

36 Zhang, Y.; Zhang, H.; Lin, G.; Chen, P.; Yuan, Y.; Tsai, K. R. Preparation, characterization and catalytic hydroformylation properties of carbon nanotubes-supported Rh-phosphine catalyst. *Appl. Catal. A: Gen.* **1999**, *187*, 213–224.

37 Zhang, A. M.; Dong, J. L.; Xu, Q. H.; Rhee, H. K.; Li, X. L. Palladium cluster filled in inner of carbon nanotubes and their catalytic properties in liquid phase benzene hydrogenation. *Catal. Today* **2004**, *93–5*, 347–352.

38 Tessonnier, J. P.; Pesant, L.; Ehret, G.; Ledoux, M. J.; Pham-Huu, C. Pd nanoparticles introduced inside multi-walled carbon nanotubes for selective hydrogenation of cinnamaldehyde into hydrocinnamaldehyde. *Appl. Catal. A: Gen.* **2005**, *288*, 203–210.

39 Ma, H.; Wang, L.; Chen, L.; Dong, C.; Yu, W.; Huang, T.; Qian, Y. Pt nanoparticles deposited over carbon nanotubes for selective hydrogenation of cinnamaldehyde. *Catal. Commun* **2007**, *8*, 452–456.

40 Li, L. J.; Khlobystov, A. N.; Wiltshire, J. G.; Briggs, G. A. D.; Nicholas, R. J. Diameter-selective encapsulation of metallocenes in single-walled carbon nanotubes. *Nat. Mater.* **2005**, *4*, 481–485.

41 Shiozawa, H.; Pichler, T.; Grüneis, A.; Pfeiffer, R.; Kuzmany, H.; Liu, Z.; Suenaga, K.; Kataura, H. A catalytic reaction inside a single-walled carbon nanotube. *Adv. Mater.* **2008**, *20*, 1443–1449.

42 Lee, J.; Kim, H.; Kahng, S. J.; Kim, G.; Son, Y. W.; Ihm, J.; Kato, H.; Wang, Z. W.; Okazaki, T.; Shinohara, H.; Kuk, Y. Bandgap modulation of carbon nanotubes by encapsulated metallofullerenes. *Nature* **2002**, *415*, 1005–1008.

43 Guan, J.; Pan, X.; Liu, X.; Bao, X. Syngas segregation induced by confinement in carbon nanotubes: A combined first-principles and Monte Carlo study. *J. Phys. Chem. C* **2009**, *113*, 21687–21692.

44 Xu, S.; Zhang, W.; Li, X.; Han, X.; Liu, X.; Bao, X. To be submitted for publication.

45 Chen, H.; Sholl, D. S. Rapid diffusion of CH_4/H_2 mixtures in single-walled carbon nanotubes. *J. Am. Chem. Soc.* **2004**, *126*, 7778–7779.

46 Blase, X.; Charlier, J. C.; De Vita, A.; Car, R.; Redlich, P.; Terrones, M.; Hsu, W. K.; Terrones, H.; Carroll, D. L.; Ajayan, P. M. Boron-mediated growth of long helicity-selected carbon nanotubes. *Phys. Rev. Lett.* **1999**, *83*, 5078–5081.

47 Czerw, R.; Terrones, M.; Charlier, J. C.; Blase, X.; Foley, B.; Kamalakaran, R.; Grobert, N.; Terrones, H.; Tekleab, D.; Ajayan, P. M.; Blau, W.; Rühle, M.; Carroll, D. L. Identification of electron donor states in N-doped carbon nanotubes. *Nano Lett.* **2001**, *1*, 457–460.

48 Garcia-Garcia, F. R.; Alvarez-Rodriguez, J.; Rodriguez-Ramos, I.; Guerrero-Ruiz, A. The use of carbon nanotubes with and without nitrogen doping as support for ruthenium catalysts in the ammonia decomposition reaction. *Carbon* **2010**, *48*, 267–276.

49 Hino, S. Electron interaction between encapsulated atoms and x-electrons in a fullerene Cage. *J. Low Temp. Phys.* **2006**, *142*, 127–132.

50 Zhang, Q.; Huang, J.; Zhao, M.; Qian, W.; Wang, Y.; Wei, F. Radial growth of vertically aligned carbon nanotube arrays from ethylene on ceramic spheres. *Carbon* **2008**, *46*, 1152–1158.

51 Philippe, R.; Caussat, B.; Falqui, A.; Kihn, Y.; Kalck, P.; Bordère, S.; Plee, D.; Gaillard, P.; Bernard, D.; Serp, P. An original growth mode of MWCNTs on alumina supported iron catalysts. *J. Catal.* **2009**, *263*, 345–358.

52 Cambaz, Z. G.; Yushin, G.; Osswald, S.; Mochalin, V.; Gogotsi, Y. Noncatalytic synthesis of carbon nanotubes, graphene and graphite on SiC. *Carbon* **2008**, *46*, 841–849.